ISSN 0036-0236, Russian Journal of Inorganic Chemistry, 2012, Vol. 57, No. 11, pp. 1436–1442. © Pleiades Publishing, Ltd., 2012.
Original Russian Text © Yu.M. Nikolenko, A.M. Ziatdinov, 2012, published in Zhurnal Neorganicheskoi Khimii, 2012, Vol. 57, No. 11, pp. 1528–1534.

SYNTHESIS AND PROPERTIES OF INORGANIC COMPOUNDS

Synthesis and Characterization of Nanographites with Chemically Modified Edges

Yu. M. Nikolenko and A. M. Ziatdinov

Institute of Chemistry, Far East Branch, Russian Academy of Sciences, pr. Stoletiya Vladivostoka 159, Vladivostok, 690022 Russia

Received August 15, 2011

Abstract—Nanographites, the structural blocks of activated carbon fibers in which the predominant part of edge carbon atoms forms covalent bonds with a chosen halogen (fluorine or chlorine), were synthesized and studied using X-ray photoelectron spectroscopy, X-ray diffraction analysis, and electron paramagnetic resonance. It was found that the formation of these bonds leads to changes in the density of states at the Fermi level and also in the values of some parameters of the spin system of current carriers of the boundary π-electron states of nanographites.

DOI: 10.1134/S0036023612110101

Nanosized carbon systems (fullerenes, nanotubes, nanohorns, etc.) and their compounds possess a set of unusual physicochemical properties, and they are promising materials for nanotechnologies [1–3]. The generalization of experimental data on these systems shows [3–6] that many of their most important electronic properties are determined by the structure of an sp^2-carbon network, which depends, in particular, on the nature and distribution of structural defects, including the edges of a nanosized carbon system. In this approach to the interpretation of the nature of electronic properties of nanosized carbon systems, nanographene and a stack of several nanographenes (nanographite) (Fig. 1), which have developed edges, become the full members of the family of promising nanosized carbon materials. On the other hand, the presence of open edges in nanographene and nanographite is a fundamental difference from the infinite network of graphene, ball-shaped fullerenes, and cylindrical carbon nanotubes with a negligibly small effect of the open ends on their properties.

Calculations showed [4–6] that the electronic structure of nanographene critically depends on the shape of its edges. A specific boundary electronic state occurs in nanographenes with zigzag edges [4, 5]. It is not inherent to macroscopic graphite and not generated by the dangling σ bonds of carbon, but it appears because of the properties of π electrons at the zigzag edges. The energy bands corresponding to this state have a partially flat structure near the Fermi level; because of this, the spectrum of the density of electronic states contains a sharp maximum [4–6]. In the calculations of the electronic structure of nanographenes with saddle-shaped edges, a boundary state of this kind does not appear [4, 5]. As for nanographene with the random structure of edges, it is impossible to theoretically reveal the characteristic details of its electronic structure near the Fermi level because of the complexity of calculations. At the same time, several independent research groups experimen-

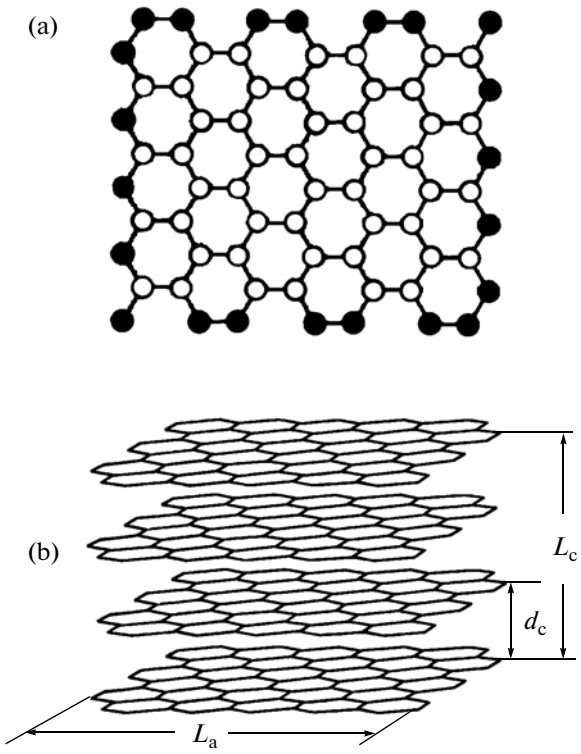

Fig. 1. Schematic diagrams of (a) idealized nanographene and (b) nanographite. The edge carbon atoms of nanographene are shown as solid circles. L_a and L_c are the dimensions of nanographite, and d_c is the distance between nanographenes.

tally demonstrated [7–9] that, indeed, the local density of electronic states near the zigzag sections of graphene edges exhibits a sharp peak near the Fermi level. Recently, it was also found [10, 11] that the nanosized islands of graphenes obtained on different substrates have predominantly zigzag edges; that is, it is likely that this shape of edges is energetically more favorable than a saddle-like shape.

The calculations of the electronic structure and magnetic properties of nanographenes showed [12–14] that they can be changed by modifying the chemical state of edge carbon atoms. In particular, the ground state of a nanographene strip, whose carbon atoms in the zigzag positions of opposite edges occur in chemically nonequivalent states, can be magnetic [13, 14]. Obviously, the development of methods for the synthesis of nanographenes and/or nanographites, in which the majority of edge carbon atoms forms chemical bonds with the chosen element (functional group), is an important stage on the way to prepare compounds of this kind.

Here, we report the results of studies on the synthesis and characterization of nanographites, in which the predominant portion of edge carbon atoms forms covalent bonds with a chosen halogen (fluorine or chlorine).

EXPERIMENTAL

Commercial polyacrylonitrile activated carbon fibers (ACFs) with a specific surface area of ~2000 m^2/g were used as the initial system of nanographites; in terms of structure, these ACFs consisted of a disordered three-dimensional network of nanographites [15]. Fluorine and chlorine were chosen as oxidizing agents because they have the smallest covalent radii among halogens.

The fluorination of ACFs was carried out by a one-zone gas transport method with the use of BrF_3, which was formed as a result of the decomposition of sodium tetrafluorobromate. The weighed portions of the fibers together with an excess amount of $Na[BrF_4]$ were placed in an airtight nickel container. Fibers with different degrees of fluorination were obtained by varying the synthesis temperature (T_{synt}) and the time of sample exposure to fluorinating agent vapor. Experimental data [16] on the fluorination of carbon materials were taken into account in deciding on T_{synt}. In the fluorination of ACFs at temperatures lower than the thermal decomposition temperature of $Na[BrF_4]$ (≈150°C), the container with the reagents was pumped out to ≈0.1 Torr before heating. At these temperatures, the ACF reacts with the gaseous products of the partial disintegration and hydrolysis of $Na[BrF_4]$. Above 150°C, the gas of BrF_3 molecules formed upon the thermal decomposition of $Na[BrF_4]$ serves as a fluorinating agent.

The samples of chlorinated ACFs for studying by X-ray photoelectron spectroscopy (XPS) and X-ray diffraction analysis were prepared at room temperature in a quartz vessel with the use of an excess amount of an oxidizing agent. The interaction of ACFs with gaseous chlorine was studied in situ by electron paramagnetic resonance (EPR) spectroscopy at room temperature. In this case, gaseous chlorine was introduced in approximately equal portions into the quartz reactor with the sample, which was placed into the resonator of the spectrometer. The EPR spectrum was measured after the addition of the next portion of chlorine. In all of the syntheses, the vessels with the fiber were evacuated to $\approx 10^{-3}$ Torr before introducing gaseous chlorine into them.

The average values of the structural parameters of graphite domains in ACFs were determined from the X-ray spectrum recorded on a D8 diffractometer (Bruker, Germany) with a Goebel mirror (CuK_α radiation; $\lambda = 0.15417$ nm). The EPR spectra of fibers were measured on a standard EMX-6.1 X-band instrument (Bruker, Germany). The intensities and g-factor values of the EPR signals of fibers and their compounds with halogens were calibrated using the intensity and the value of $g = 2.002293 \pm 0.000003$ of the EPR signal of a LiF:Li reference sample, respectively. The chemical bonds and element concentrations in the test samples were determined by XPS from the spectra measured on an ES-2401 electron spectrometer (EZAN, Chernogolovka, Russia) with the use of nonmonochromatic AlK_α radiation. In the course of the measurements, the vacuum in the energy analyzer of the spectrometer was maintained at a level of $\approx 6 \times 10^{-8}$ Torr. The binding energies (E_b) of core electrons were measured with reference to the Fermi level of the spectrometer. The possible sample charging effect was not considered; that is, the scale of E_b was not corrected on going from sample to sample. The concentrations of the elements were calculated from the photoelectron spectra taking into account the photoionization cross sections and the asymmetry of the wave functions of core electrons [17, 18], the exit directions of detected photoelectrons, and the transmission function of the analyzer. The concentrations of chemical elements in the samples were evaluated relative to the total amount of carbon with an error of no higher than 20% [18]. If necessary, the experimental spectra were deconvoluted with the use of the XPSPEAK 4.1 freeware. When a sample was arranged in the spectrometer, a dry box directly connected to the sample introduction system was used to prevent it from contact with atmospheric moisture.

Activated carbon materials other than consolidated nanographite particles can contain a small impurity fraction of aliphatic carbon, which can also react with the oxidizing agent. In special studies of the mass spectra of residual gases in a high-vacuum chamber, we found that the prolonged heating of the initial ACF at a temperature higher than 400°C with simultaneous pumping to a high vacuum led to the almost complete removal of the free aliphatic impurity fraction from the fiber. On the heating of the fiber to 800–850°C, the

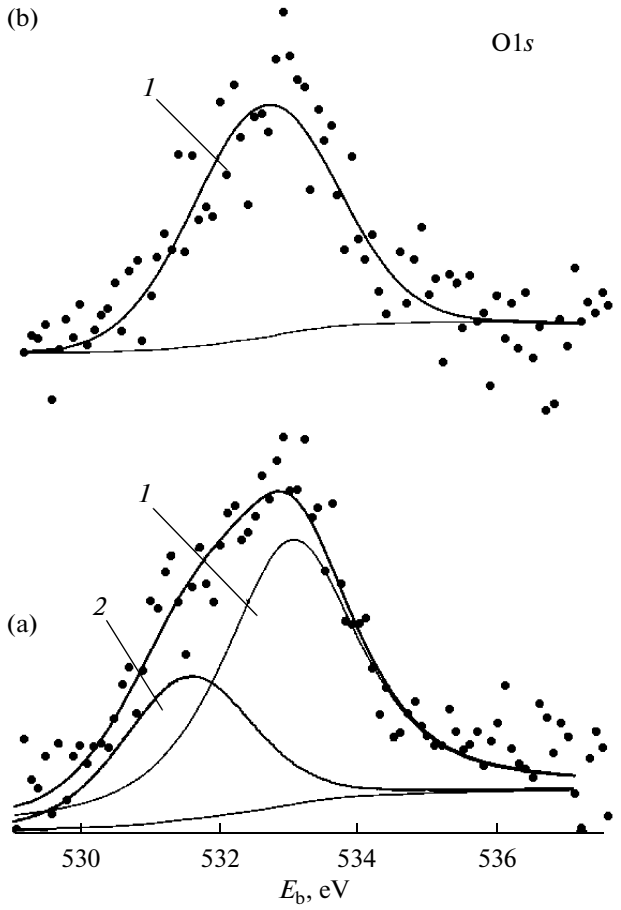

Fig. 2. The O1*s* XPS spectra of (a) the initial ACF and (b) the ACF annealed at 850°C: (*1*) the oxygen line of –OR groups (R is a hydrocarbon radical or H) and (*2*) the oxygen line of the carbonyl group.

composition of oxygen-containing functional groups also changed (Fig. 2) and the relative concentration of oxygen in the sample decreased (from ≈10 to ≈3%). With consideration for these data, only samples after this preliminary purification were used in all of the studies on the fluorination and chlorination of ACFs.

RESULTS AND DISCUSSION

The sizes of graphite particles—the structural blocks (domains) of ACFs—were estimated from the reflection parameters of the X-ray diffraction spectrum. After subtracting the contribution of background scattering, the X-ray diffraction spectrum of ACF can be represented as the sum of three Loretzians corresponding to the (002), (100), and (101) reflections (Fig. 3). The average interlayer distance $d_c \approx$ 0.384 nm and the average domain size of graphite in the direction perpendicular to the layers $L_c \approx 1$ nm were evaluated from the position and width of the (002) reflection, respectively, with the use of standard calculation methods. Analogously, the average domain

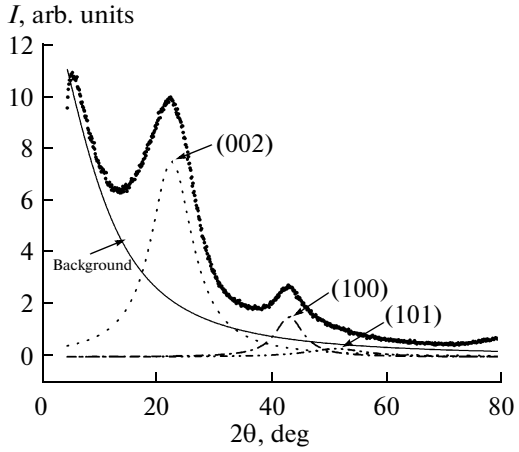

Fig. 3. X-ray diffraction spectrum of ACF and its deconvolution into three Lorentzians corresponding to the (002), (100), and (101) reflections.

size of graphite in the plane of carbon layers $L_a \approx 1.61$ nm was evaluated from the width of the (100) reflection. Thus, in the test ACFs, the domains of graphite have nanometer sizes both along and perpendicular to carbon layers. These data indicate that nanographites consist of three or four nanographenes, the distance between which is substantially greater than the distance between the carbon layers in macroscopic ordered graphite (0.335 nm).

The spectrum of the C1*s* electrons of the initial ACF exhibited an intense asymmetric line with $E_b = 284.3 \pm 0.1$ eV, which is characteristic of conducting carbon materials (Fig. 4a). Along with $\pi \rightarrow \pi^*$ excitations, the low-intensity signals of carbon atoms bound to different residual oxygen-containing functional groups participate in the formation of the carbon spectrum profile on the side of high E_b with respect to the main peak.

An analysis of chemical bonds and element concentrations in the products of ACF reactions with oxidizing agent vapors at $T_{synt} < 150$°C showed that, at these temperatures, the reaction time is the main factor responsible for the degree of fluorination/oxidation of the fiber. The amount of oxygen in the end reaction product increased by a factor of 3–4, as compared with the oxygen content of the initial purified fiber; this fact suggests its participation in the oxidation of nanographites. Obviously, the increase in the oxygen content in the course of oxidation was due to the presence of oxygen as a constituent of the fluorinating/oxidizing gas mixture caused by the prehistory of $Na[BrF_4]$. In this case, the spectrum of O1*s* electrons became similar to the spectrum of oxygen in the initial ACF, which did not undergo preliminary purification. The C1*s* spectrum of the product of the reaction of ACF with oxidant vapors also exhibited lines that can be attributed to carbon atoms bound to fluorine and oxygen-containing functional groups on the

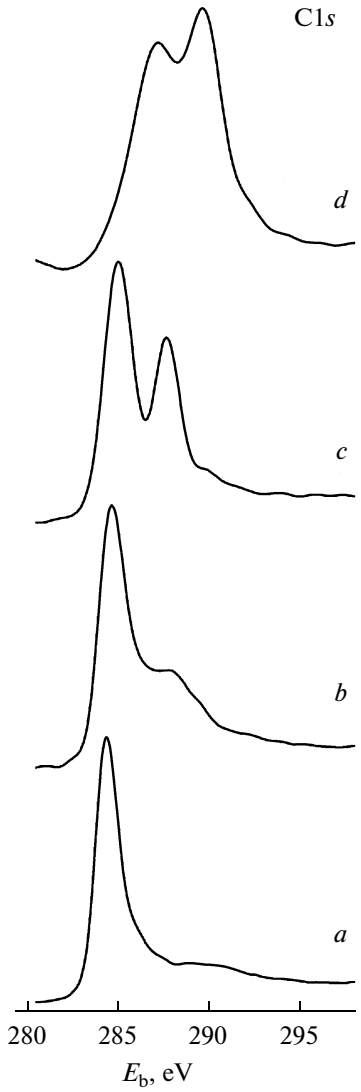

Fig. 4. Smoothed C1*s* XPS spectra of (a) the initial ACF and the ACFs fluorinated at (b) 100, (c) 155, and (d) 300°C.

side of high binding energies relative to the main asymmetric component (Fig. 4b).

At T_{synt} > 150°C, the degree of ACF fluorination mainly depends on temperature. At these synthesis temperatures, the oxygen content of the sample remained unchanged in the course of its fluorination. A line with E_b greater than that of the main asymmetric component of the spectrum by ≈2.7 eV was present in the C1*s* spectrum of ACF fluorinated at ≈155°C (Fig. 4c); this makes it possible to attribute it to the carbon atom that forms a bond with one fluorine atom. The integrated intensity of this line is 25–30% of the total integrated intensity of the C1*s* spectrum, and it correlates with the percentage of edge carbon atoms in idealized nanographite (Fig. 1).

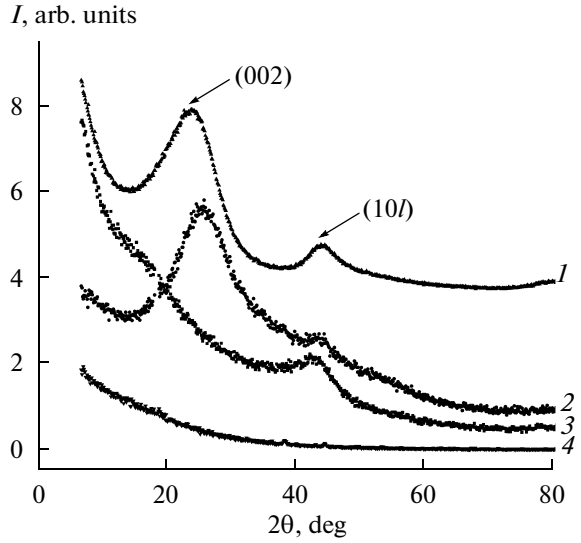

Fig. 5. X-ray diffraction spectra of (*1*) the initial ACF and the ACFs fluorinated at (*2*) 100, (*3*) 155, and (*4*) >300°C.

The characteristics of the XPS spectra of the fibers fluorinated at ~300°C are substantially different from those of the spectra of samples fluorinated at lower temperatures. In particular, the lines of all elements in them are shifted toward the side of high energies. This fact suggests the charging of the samples as a result of photoelectron emission, which can be explained by a worsening of their conducting properties. This is also evident from the symmetry of all of the C1*s* spectrum components of the end reaction product, which is characteristic of nonconducting carbon compounds. Note that, in this sample, the C1*s* spectrum components that correspond to the carbon atoms not bound to fluorine and bound to one fluorine atom are similar in intensity (Fig. 4d). The above facts suggest that ACF fluorination at ~300°C leads to the formation of nonconducting nanographite compounds, which are similar in composition to digraphite monofluoride $(C_2F)_n$; according to Watanabe et al. [19], digraphite monofluoride consists of corrugated pairwise-crosslinked layers of sp^3-hybridized carbon.

The X-ray diffraction spectra of the initial fibers and the fibers fluorinated at 100°C (Fig. 5, curves *1* and *2*, respectively) are qualitatively similar, and they contain the (002) reflection and the unresolved (10*l*) reflection; that is, fluorination at the specified temperature does not lead to a substantial change in the structure of nanographites. Nanographenes were present in the samples fluorinated at ≈155°C (Fig. 5, curve *3*); however, the average distance and the spread of distances between them were much greater than those in the initial sample. Only trace laminar structures were detected in the ACFs fluorinated at T_{synt} ≈ 300°C, whereas reflections characteristic of nanographites were absent at temperatures much higher than 300°C (Fig. 5, curve *4*).

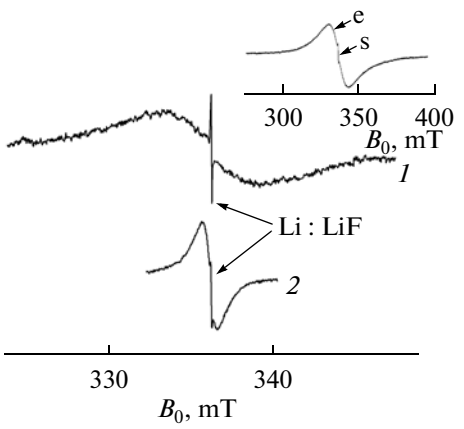

Fig. 6. EPR spectra of (*1*) the initial ACF and (*2*) the ACF fluorinated at room temperature (the narrow signal with $g = 2.002290 \pm 0.000004$ belongs to the conduction electrons of lithium nanoparticles in the LiF:Li reference sample). Inset: EPR spectrum of the initial ACF with no reference sample at −15°C (e and s refer to the signals of current carriers and localized spins, respectively).

The EPR spectra of both the initial ACF and the fibers fluorinated at $T_{synt} \approx 300$°C contain a broad and a narrow signal (Fig. 6). The broad and narrow signal intensity does not depend on temperature and varies with temperature according to the Curie law. These data make it possible to interpret the wide signal as the spin resonance of conduction electrons (CESR) and to consider the narrow signal as a localized spin resonance. Ziatdinov [20] found that, in the test ACFs, the current carriers of the edge π-electron states of nanographites make the main contribution to CESR. In the samples fluorinated at temperatures of about 300°C or higher, only the localized spin resonance was observed.

The integrated intensity and the width of the CESR signal decrease with the degree of ACF fluorination. Thus, in the fiber fluorinated at ≈155°C, they were smaller than those in the initial samples by factors of 1.3 and ≈3, respectively. Because the integrated intensity and the width of the CESR signal are proportional to the density of states at the Fermi level and the rate of the spin relaxation of current carriers, respectively [21], it is obvious that, from the decrease of these parameters upon the fluorination of fibers, it follows that the above two parameters of the system of current carriers also decrease in this case. The *g*-factor value of 2.0027 ± 0.0001 for the CESR signal in the initial fiber increased with the degree of its fluorination to reach 2.0032 ± 0.0002 in the samples fluorinated at ≈155°C. The absence of the CESR signal from the samples fluorinated at temperatures of about 300°C or higher is indicative of a substantial change in their electronic structure at the specified synthesis temperatures; this is consistent with the above data on the studies of the test samples by XPS and X-ray diffraction analysis.

The EPR signal due to localized spins was present in all of the fluorinated fibers. Its *g*-factor value of 2.0027 ± 0.0001 was independent of the degree of fluorination of the sample; that is, it coincided with the *g*-factor value of the CESR signal in the initial fiber within the limits of experimental error. According to EPR-spectroscopic data, the concentration of localized spins in ACFs nonmonotonically depends on the degree of fluorination: in the fibers fluorinated at ~155 or ≈300°C, it was ≈60% lower or several times higher than that in the initial sample, respectively.

From the XPS and X-ray diffraction data for ACFs fluorinated at ≈155°C, it follows that fluorine predominantly forms covalent bonds with the edge carbon atoms of nanographites at the above t_{synt}. Therefore, we assume that this factor initiates changes in the density of states at the Fermi level and some characteristics of the spin system of the current carriers of the edge π-electron states of nanographites, which were detected by EPR spectroscopy. The decrease in the concentration of localized spins observed in this case can be explained by the formation of bonds between fluorine and edge carbon atoms with dangling σ bonds. Note that the conclusion on the onset of the fluorination of nanographites at the peripheral atoms is also consistent with the results of the theoretical calculations of the phase sequence of nanographene fluorination [12].

It is likely that, in the samples fluorinated at ≈300°C or higher, the orbitals of carbon atoms in the interior of nanographites are rearranged to sp^3-type orbitals. Three of these orbitals in each carbon atom participate in the formation of a corrugated carbon network, and the fourth orbital participates in the formation of a covalent bond with the fluorine atom or remains free; that is, this is a dangling σ bond. An increase by several times in the concentration of localized spins at the fluorination temperatures under discussion can be explained by the presence of such dangling bonds. The presence of dangling σ bonds in a sample also indicates that, unlike $(C_2F)_n$ [19], the corrugated layers of carbon are not completely crosslinked with each other in this sample.

The C1*s* spectrum profile of chlorinated ACF has a singularity shifted by 1.5–1.7 eV relative to the main maximum on the scale of binding energies (indicated by an arrow in Fig. 7). For explaining its nature, we carried out a computer simulation of the C1*s* spectra in accordance with a published procedure [22]. This approach to the simulation of spectra is based on the approximate equality of the line intensities of the chemical elements (with consideration for corresponding corrections) that participate in the formation of a chemical bond. The C1*s* spectrum of the initial ACF was simulated in accordance with this procedure with the use of the shifts of the binding energies (ΔE_b) of the C1*s* electrons of carbon bound to different functional groups with respect to the E_b of these electrons in saturated hydrocarbons [18] and the integrated intensity of a single line due to O1*s* electrons in

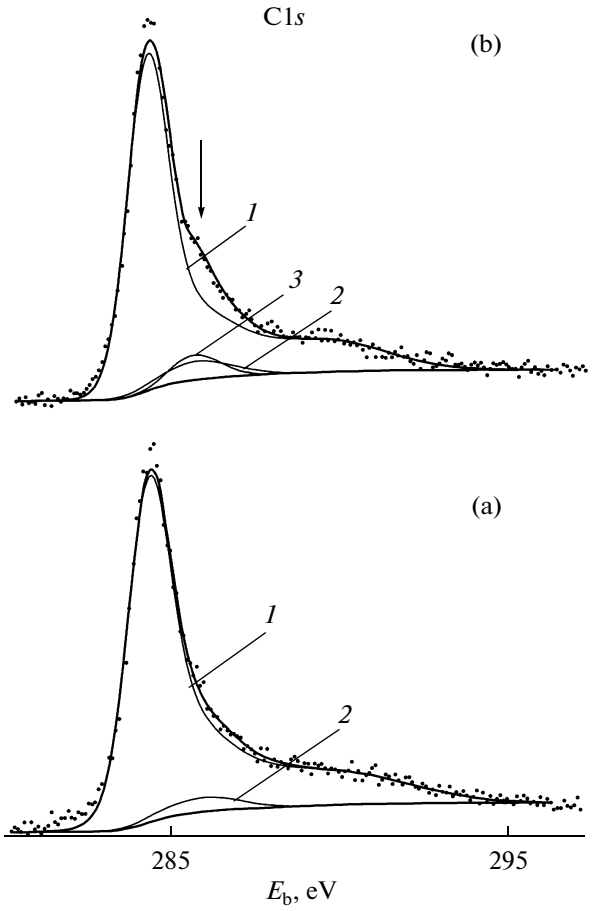

Fig. 7. The C1*s* XPS spectrum of ACF (a) before and (b) after chlorination: (*1*) spectrum component caused by the carbons of nanographites, the aliphatic fragments of the fiber, surface hydrocarbon impurities, and lines due to the $\pi \rightarrow \pi^*$ excitation; (*2*) spectrum component corresponding to the carbon of C–OR groups, where R is a hydrocarbon radical or H; and (*3*) spectrum component corresponding to the carbon bound to chlorine.

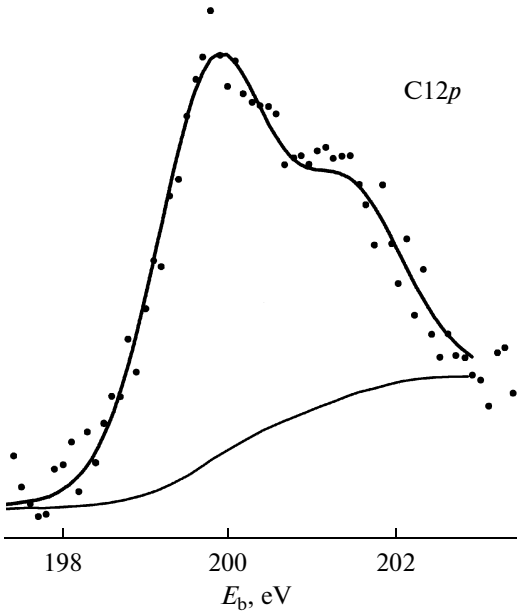

Fig. 8. The Cl2*p* XPS spectrum of chlorinated ACF.

the spectrum of the fiber. On the assumption that oxygen completely belongs to functional groups chemically bound to the ACF, the above analytical procedure made it possible to separate a component due to carbon bound to oxygen in groups like C–OR ($\Delta E_b = 1.6$ eV), where R is a hydrocarbon radical or H, in the C1*s* spectrum (Fig. 7a). The experimental C1*s* spectrum of chlorinated ACF is adequately simulated upon the addition of a component corresponding to carbon bound to chlorine ($\Delta E_b = 1.5$ eV [18]) (Fig. 7b), whose intensity is determined by the spectrum intensity of chlorine 2*p* electrons in the fiber (Fig. 8). The maximum of the Cl2*p* spectrum is characterized by $E_b = 199.8 \pm 0.1$ eV, which is close to the binding energy of the corresponding electrons of chlorine covalently bound to carbon in a number of organic compounds [18]. The position in the scale of energies and the intensity of the chlorine signal were stable even upon the heating of the sample in a vacuum to ≈150°C. These facts suggest the covalent binding of chlorine with carbon. The absence of the sample charging effect from the chlorinated fiber indicates the retention of its conducting properties. According to X-ray diffraction data, the chlorination of fibers at room temperature does not substantially change the structure of nanographites and the corrugation of the constituent nanographenes. Taking into account all of these data and the almost complete removal of aliphatic fragments from the sample in the course of its preliminary high-vacuum evacuation at a high temperature, we believe that, under the chosen synthesis conditions, chlorine forms covalent bonds predominantly with the peripheral atoms of nanographites.

As the number of chlorine portions admitted into the reactor with ACF was increased, the CESR signal monotonically narrowed to ≈0.8 mT (Fig. 9). In this case, its *g*-factor value increased to 2.0032 ± 0.0002 and intensity decreased by ≈20%. Taking into account the data of the XPS and X-ray diffraction studies of chlorinated ACFs, we consider that the reason for the above changes in the CESR signal parameters, as well as in the experiments on the fluorination of ACFs, is the formation of covalent bonds between chlorine and the edge carbon atoms of nanographites. As the ratio between the chlorine and carbon contents was increased, the concentration of localized spins, which was determined by EPR spectroscopy, monotonically decreased by ≈40%; this fact is indicative of the formation of bonds between chlorine and edge carbon atoms with dangling σ bonds.

Thus, we found conditions for the fluorination of ACF under which fluorine forms covalent bonds predominantly with the edge carbon atoms of nanographites (the structural blocks of the fiber) even before the

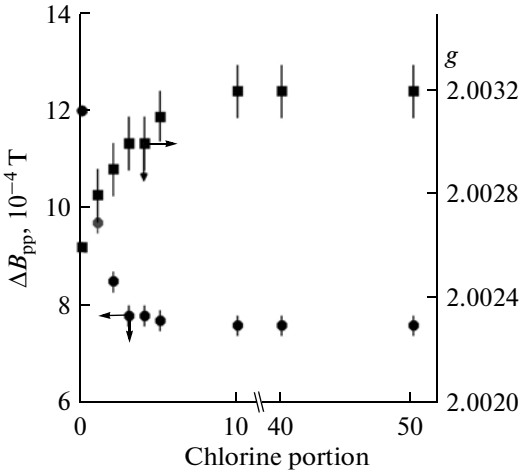

Fig. 9. The *g*-factor values and the CESR signal widths (ΔB_{pp}) as functions of the number of chlorine portions admitted into the reactor with ACF.

onset of the formation of these bonds with the carbon atoms of the interior of nanographites. We found that the treatment of ACFs with chlorine molecules at room temperature also leads to the formation of covalent bonds between chlorine and the edge carbon atoms of nanographites without the formation of such bonds with carbon atoms in the interior of nanographites. The formation of covalent bonds between a halogen and the edge carbon atoms of nanographite leads to changes in the density of states of current carriers at the Fermi level, the *g*-factor values, and the rate of spin relaxation of the current carriers of edge π-electron states. The result obtained is an important stage on the way to the preparation of nanographenes and nanographites with different chemical states of opposite edges; according to calculations [12–14], the ground state of these species can be magnetic.

ACKNOWLEDGMENTS

We are grateful to Cand. Sci. (Chem.) V.V. Kainara for his assistance in performing the EPR-spectroscopic studies of chlorinated ACFs. This work was supported in part by the Russian Foundation of Basic Research (project no. 08-03-00211-a) and the Presidium of the Far East Branch of the Russian Academy of Sciences (project no. 09-I-P18-07).

REFERENCES

1. A. Kruger, *Carbon Materials and Nanotechnology* (Wiley-VCH, Weinheim, 2010).
2. T. Makarova and F. Palacio, *Carbon Based Magnetism* (Elsevier, Amsterdam, 2006).
3. M. S. Dresselhaus, G. Dresselhaus, and P. C. Ekland, *Science of Fullerenes and Carbon Nanotubes* (Academic Press, New York, 1996).
4. M. Fujita, K. Wakabayashi, K. Nakada, and K. Kusakabe, J. Phys. Soc. Jpn. **65**, 1920 (1996).
5. K. Nakada, M. Fujita, G. Dresselhaus, and M. S. Dresselhaus, Phys. Rev. B **54**, 17954 (1996).
6. T. Enoki, Y. Kobayashi, and K. I. Fukui, Int. Rev. Phys. Chem. **26**, 609 (2007).
7. Z. Klusek, W. Kozlowski, Z. Waqar, et al., Appl. Surf. Sci. **252**, 1221 (2005).
8. Y. Kobayashi, K. Fukui, T. Enoki, et al., Phys. Rev. B **71**, 193406 (2005).
9. Y. Niimi, T. Matsui, H. Kambara, et al., Appl. Surf. Sci. **241**, 43 (2005).
10. M. Yamamoto, S. Obata, and K. Saiki, Surf. Interface Anal. **42** (8), 1637 (2010).
11. G. M. Rutter, N. P. Guisinger, J. N. Crain, et al., Phys. Rev. B **81**, 245408 (2010).
12. R. Saito, M. Yagi, T. Kimura, et al., J. Phys. Chem. Solids **60**, 715 (1999).
13. K. Kusakabe and M. Maruyama, Phys. Rev. B **67**, 092406 (2003).
14. M. Maruyama, K. Kusakabe, S. Tsuneyuki, et al., J. Phys. Chem. Solids **65**, 119 (2004).
15. H. Marsh and F. Rodrigez-Reinoso, *Activated Carbon* (Elsevier, Amsterdam, 2006).
16. G. Nanse, E. Papirer, P. Fioux, et al., Carbon **35**, 175 (1997).
17. J. H. Scofield, J. Electron Spectr. Relat. Phenom. **8**, 129 (1976).
18. V. I. Nefedov, *X-ray Photoelectron Spectroscopy of Chemical Compounds* (Khimiya, Moscow, 1984) [in Russian].
19. N. Watanabe, T. Nakajima, and H. Touhara, *Graphite Fluorides* (Elsevier, Amsterdam, 1988).
20. A. M. Ziatdinov, Ross. Khim. Zh. **47** (5), 5 (2004).
21. J. Weil and J. R. Bolton, *Electron Paramagnetic Resonance: Elementary Theory and Practical Applications* (Wiley-Interscience, New Jersey, 2007).
22. Yu. M. Nikolenko, A. K. Tsvetnikov, T. Yu. Nazarenko, and A. M. Ziatdinov, Russ, J. Inorg. Chem. **41**, 721 (1996).